Sensitivity of a mechanistic photosynthesis model to tropical Andean species and environments

Sebastián González-Caro[1,2]; Mirindi Eric Dusenge[3]; Zorayda Restrepo[4]; Andrew J. F. Cox[5], Ian P. Hartley[1]; Patrick Meir[6]; Adriana Sánchez[7]; Daniel Ruiz-Carrascal[8]; Lina M. Mercado[1,9]

[1]Faculty of Environment, Science and Economy, University of Exeter, Exeter, United Kingdom
[2]Instituto de Biología, Universidad de Antioquia, Medellín, Colombia
[3]Research School of Biology, Australian National University, Canberra, Australia
[4]COLTREE Corporation, Medellin, Colombia
[5]Met Office, Exeter, United Kingdom
[6]School of Geosciences, University of Edinburgh, Edinburgh, United Kingdom
[7]Department of Biological Sciences, Universidad del Rosario, Bogotá, Colombia
[8]Sistema de Alertas Tempranas de Medellín y el Valle de Aburrá, SIATA, , Medellin, Colombia
[9]UK Centre for Ecology and Hydrology, Crowmarsh-Gifford, Wallingford, United Kingdom

Correspondence to: Sebastián González-Caro (sebastian.gonzalez.caro@gmail.com)

Abstract. Andean tropical montane forests are highly biodiverse ecosystems with a carbon storage capacity comparable to lowland forests. However, their response to climate change remains uncertain, as species photosynthesis depends on their thermal acclimation capacity. This study evaluates the variability of photosynthetic traits across montane and lowland tree species using a leaf level photosynthesis model and data from a transplant experiment across three elevations varying in their mean annual temperatures (14°C, 22°C, and 26°C) in the tropical Andes. Six montane species and two lowland species were analyzed to assess photosynthetic responses to environmental conditions. We find that intraspecific variability in photosynthetic parameters, such as the apparent maximum carboxylation capacity (V_{cmax}) and the apparent maximum electron transport rate (J_{max}), is key to accurately model photosynthesis in these ecosystems. Apparent V_{cmax} was identified as the primary determinant of diurnal variations in photosynthesis, especially under varying thermal environments. Additionally, stomatal conductance (g_1) was highly variable and responded to vapor pressure deficit (*VPD*), suggesting that stomatal regulation is crucial for adaptation to environmental changes. Sensitivity analysis revealed that at higher altitudes (14°C), photosynthetically active radiation (PAR) and temperature were the main limiting factors for photosynthesis, while at lower altitudes (22°C), VPD was the dominant factor. Finally, the study demonstrates that the common use, within global vegetation models, of average parameters from lowland species to simulate montane forest is inadequate as such parameterizations tend to underestimate montane forest photosynthesis by up to 65%. It is also recommended that vegetation models incorporate both intra- and interspecific variability to improve predictions of the carbon cycle in tropical Andean forests and their response to climate change.

1. Introduction

Tropical montane forests are among the planet's most biodiverse ecosystems (Myers et al., 2000) and play a critical role in global carbon storage. Large-scale syntheses have shown that these ecosystems store substantial amounts of aboveground carbon, sometimes comparable to that of tropical lowland forests when differences in temperature and productivity are considered (Cuni-Sánchez et al., 2021; Duque et al., 2021). In the Andes, for example, Duque et al. (2021, Table 1) reported a monotonic decline in aboveground carbon stocks—from about 89 Mg C ha^{-1} at 500–1200 m to 59 Mg C ha^{-1} at 2800–3600 m a.s.l.—yet these values remain high relative to the cooler, less productive conditions under which they occur. Such evidence suggests that, although biomass decreases with elevation, tropical montane forests maintain unexpectedly large carbon stores, likely supported by physiological adjustments that sustain carbon assimilation under cold and cloudy environments (Fyllas et al., 2017; Girardin et al., 2010). While biomass per unit land area integrates processes such as recruitment, mortality, and allocation, these processes are ultimately constrained by carbon assimilation at the leaf level (Bahar et al., 2017; Malhi et al., 2017; van de Weg et al., 2014). Photosynthesis therefore defines the physiological potential for carbon gain, and its capacity to acclimate to temperature may explain how tropical montane forests maintain relatively high carbon stocks despite cooler climates. Experimental evidence further indicates that photosynthetic capacities of tropical montane and lowland trees are similar when both are grown under comparable mid-elevation conditions (Dusenge et al., 2021; Cox et al., 2023; Dusenge et al., 2025). However, when evaluated in their native environments—cooler high-elevation or warmer low-elevation sites—photosynthetic capacities diverge. This pattern supports the idea that tropical montane species can acclimate, at least partially, to local thermal conditions, providing a mechanistic explanation for the stability of montane forest productivity under a warming climate.

Such thermal plasticity of photosynthetic capacity could enable montane species to sustain tree growth and aboveground biomass accumulation at rates in highland forests comparable to those in lowland forests. Nevertheless, it remains uncertain whether this physiological acclimation is sufficient to maintain growth and photosynthetic functioning of montane species under the warmest experimental conditions they experience. Observational studies in tropical Andean and Afromontane forests suggest that species composition has shifted in response to recent warming, likely driven by selective mortality of montane tree species to increased mortality at lower elevations (Duque, Stevenson, and Feeley, 2015; Fadrique et al., 2018). Specifically, lowland tree species have been observed migrating upslope, while montane species experience range contractions due to high mortality at the warmest margins of their geographical distribution—an effect known as thermophilisation (Duque, Stevenson, and Feeley, 2015; Fadrique et al., 2018; Cuni-Sanchez et al., 2024). This mortality is thought to result from thermal limitations to photosynthesis and associated carbon imbalance under extreme warming. At temperatures near or above the optimum for photosynthesis, enzymatic activity declines and photorespiration increases, reducing net carbon gain (Mercado et al., 2018). When this reduction in carbon assimilation persists, it can lead to growth suppression and eventually higher mortality for species living at the warmest margins of their distributions, where physiological acclimation may no longer compensate for thermal stress. To better assess species' ability to maintain photosynthetic function under rapidly changing

conditions, characterised by accelerated warming, reduced cloud immersion, and altered moisture regimes in tropical montane regions (Fadrique et al., 2018; Duque et al., 2021), a combination of experimental and modeling is required, particularly in the context of increasing environmental extremes.

Most global vegetation, land surface, and Earth system models most vegetation models currently represent both montane and lowland tropical forests using a single plant functional type, which neglects the physiological diversity and thermal specialization of species across elevations (Fisher et al., 2018; Harper et al., 2018; Poulter et al., 2011). But it is now known that species from these forests differ in key photosynthetic traits and that these traits are plastic in response to warming (Cox et al., 2024; Dusenge et al., 2021; Kumarathunge et al., 2019). Furthermore, these models scale up leaf-level physiological processes, such as photosynthesis, respiration, stomatal conductance and transpiration, from leaf to canopy level which is then used to perform simulations at site, regional and global levels. Therefore, model parameterizations and evaluations at the leaf level are crucial for advancing model accuracy. Photosynthesis is one of the key processes at the heart of these models. However, photosynthetic traits employed in land surface and Earth system model predictions are commonly averaged across species (Fisher et al., 2018; Oliver et al., 2022; Poulter et al., 2011), and the (interspecific and intraspecific) variance is rarely considered in such large scale process-based models. This simplification can be problematic if systematic differences in key physiological parameters exist among species groups, for example the differential responses to warming observed for tropical montane versus lowland trees (Cox et al., 2023; Mujawamariya et al., 2023). While it is neither feasible nor necessary to parameterize every species in these highly diverse forests, identifying consistent physiological contrasts among major functional groups can improve model realism without excessive complexity. Given the substantial contribution of tropical montane forests to global carbon cycling (Cuni-Sanchez et al., 2021; Duque et al., 2021), there is a need for leaf-level models parameterized and evaluated with montane tropical data to inform large-scale models and produce more reliable estimates of regional carbon budgets and their responses to future climate.

Tropical Andean forests are known to harbour high biodiversity (Myers et al., 2010) with communities composed of species that differ widely in their functional traits and environmental tolerances (Fyllas et al., 2017; González-Caro et al., 2023). Consequently, substantial interspecific variation in photosynthetic traits can be expected within any given location. Such variation implies that the use of single average parameter values in models (Knauer et al., 2023; Oliver et al., 2022) may obscure the actual diversity of physiological responses to environmental conditions. Andean species are exposed to a variety of thermal conditions because of the large range in environmental conditions across elevational bands, including within a single location through large diurnal variation (Martínez et al., 2011; van de Weg et al., 2014). This is also reflected in the large thermal ranges of some abundant species which can be found within a natural mean annual temperature span of up to 15 to 20 degrees (Montaño-Centellas et al., 2024). Additionally, fluctuating cloud and wind regimes create constantly changing environmental conditions, making it impractical for plants to maintain photosynthesis at optimal levels at all times. All these conditions could promote both high intraspecific variation and acclimation of photosynthetic traits in Andean tree species (Bahar et al., 2017; Cox et al., 2023, 2024). Empirical observations and photosynthesis models can be used to assess the effect of intraspecific variance of photosynthetic traits on photosynthesis of Andean forests.

Mechanistic models, such as the widely used C_3 photosynthesis model developed by *Farquhar*, *von Caemmerer*, and *Berry* (hereafter referred to as the *FvCB* model), effectively describe photosynthesis by integrating the biochemical drivers of this process along with the response of stomatal conductance to leaf-to-air vapor pressure deficit (Farquhar et al., 1980). The *FvCB* model is useful to analyse the impact of environmental drivers on photosynthesis by varying parameters that are closely associated with enzymatic activity, primarily related to Rubisco during the CO_2 assimilation process. Previous modelling efforts have applied this framework to quantify the limitations of photosynthesis imposed by temperature, vapor pressure deficit (*VPD*), and light availability in tropical forests (Mercado et al., 2018; Smith et al., 2019). However, these studies have been largely based on lowland species, and the extent to which montane trees differ in their photosynthetic sensitivity to these environmental drivers remains poorly understood. Addressing this gap requires parameterisations derived from direct field measurements across contrasting elevations. Given the high environmental heterogeneity of tropical montane forests and the potentially plastic response capabilities of their native species (Cox et al., 2023), the parameterisation of the *FvCB* model must therefore be approached cautiously to accurately capture both species response variability and environmental heterogeneity (Blonder et al., 2020).

In this study, we combined the FvCB model with field-based data from a transplant experiment in the tropical Andes to address two main questions: i) What is the effect of intraspecific variation in plant physiological traits on photosynthetic performance and on the differences between montane and lowland species? We hypothesised that intraspecific variation in physiological traits contributes significantly to differences in leaf-level photosynthetic capacity among tropical montane tree species. Specifically, we predicted that species with higher photosynthetic capacity (e.g., higher V_{cmax} and J_{max}) would maintain greater carbon assimilation rates under warmer conditions. ii) How do photosynthesis and related traits respond to environmental conditions at different sites, and how do these responses influence forest-level assimilation depending on the plant functional type (montane vs. lowland species)? We further hypothesised that environmental drivers such as air temperature, vapour pressure deficit (*VPD*), and light availability (*PAR*) exert distinct and interacting effects on photosynthesis across thermal regimes. Accordingly, we predicted that temperature would be the dominant limiting factor at high-elevation (cool) sites, whereas *VPD* would impose stronger constraints at low-elevation (warm) sites. Finally, we expected that including both plant functional types in simulations would increase overall assimilation rates and reduce their temporal variability within a site.

2. Material and Methods

We used the *FvCB* processes-based C_3 photosynthesis model along with leaf gas-exchange data from trees planted in the field to calibrate and evaluate photosynthesis models using different parameterisationsfor montane and lowland tree species. Subsequently, we investigate the sensitivity of simulated photosynthesis to key model parameters and various environmental conditions (Figure 1).

2.1. Common garden transplant

The experiment is based on the transplant of eight dominant tropical Andean species across two sites at different elevations (1500m and 2500m), where mean annual temperatures (14°C and 22°C) covaries with elevation but was not manipulated independently. The tree species are divided into two groups (Table 1): six montane tree species that naturally inhabit montane forests above 2000m (where mean air temperatures range from 10-22°C in their native distributions) were transplanted to the lower-elevation site with warmer temperature (22°C). these conditions represent at the warm extreme of their thermal ranges and simulate the scenarios where range retractions of montane species have been reported in Andean forests (Duque *et al.*, 2015; Fadrique *et al.*, 2018). Conversely two lowland tree species that inhabit foothill forests below 1000m (air temperatures ranging from 22-35°C) were transplanted to high elevations/cooler temperatures (14°C) to simulate upslope migration from the lowlands (Duque et al., 2015; Fadrique et al., 2018). Twenty-four saplings per species per site (total of trees planted per site n=360) were planted between December 2018 and January 2019 under common soils extracted from a nearby location to the 14°C experimental site (i.e., the soils transported to each experimental site, 400 Kg of soil used to plant each tree in soil pits of 0.32m^3) and were continuously watered to remove drought confounding effects.

2.2 Photosynthesis model

The *FvCB* model is a key tool for interpreting leaf gas exchange observations and for modelling photosynthesis. Its central function is to simulate photosynthesis reactions to changes in [CO_2] concentrations inside the leaf, and it can adjust for enzymatic reaction temperature-dependence with appropriate parameter settings (Medlyn et al., 2002). The model represents net [CO_2] assimilation rate (A_n expressed in mmol m^{-2} s^{-1}) as the difference between the minimum of two limiting photosynthetic rates: the Rubisco-limited rate (A_c expressed in mmol m^{-2} s^{-1}), which depends on the apparent maximum rate of Rubisco carboxylation (V_{cmax}), and light limited rate (A_j, expressed in mmol m^{-2} s^{-1}) which is related to the apparent maximum electron transport rate (J_{max}), minus the leaf respiration in the dark (R_d expressed in mmol m^{-2} s^{-1}):

$$A_n = \min(A_c, A_j) - R_d \quad (1)$$

Stomatal conductance is incorporated using the (Medlyn et al., 2011) model as applied in Lin et al (2015):

$$g_s = 1.6 \left(1 + \frac{g_1}{\sqrt{D}}\right) \cdot \left(\frac{A_n}{C_a}\right) \quad (2)$$

The model describes the diffusion of CO_2 through mesophyll layers and the stomata response to leaf to air vapor pressure difference (D expressed in kPa). C_a (in ppm) is CO_2 concentration at the leaf surface and g_1 (kPa$^{0.5}$) is a proxy for the plant water use strategy with small g_1 values indicating a conservative water use and large g_1 indicating the opposite (Lin et al., 2015).

2.3. Field leaf-level data and model application

We used gas exchange measurements from juvenile tropical Andean trees planted as part of a common garden transplant experiment in the Colombian Andes to derive parameters for the *FvCB* model. The experiment is based on the transplant of eight dominant tropical Andean species across two sites at different elevations (1500m and 2500m), where mean annual temperatures (14°C and 22°C) covaries with elevation but was not manipulated independently. The species are divided into two groups: six montane tree species that naturally inhabit montane forests above 2000m (where mean air temperatures range from 10-22°C in their native distributions) were transplanted to the lower-elevation site with warmer temperature (22°C). these conditions represent at the warm extreme of their thermal ranges and simulate the scenarios where range retractions of montane species have been reported in Andean forests (Duque *et al.*, 2015; Fadrique *et al.*, 2018). Conversely two lowland tree species that inhabit foothill forests below 1000m (air temperatures ranging from 22-35°C) were transplanted to high elevations/cooler temperatures (14°C) to simulate upslope migration from the lowlands (Duque et al., 2015; Fadrique et al., 2018). Twenty-four saplings per species per site (total of trees planted per site n=360) were planted between December 2018 and January 2019 under common soils extracted from a nearby location to the 14°C experimental site (i.e., the soils transported to each experimental site, 400 Kg of soil used to plant each tree in soil pits of $0.32m^3$) and were continuously watered to remove drought confounding effects.

We used leaf-level photosynthetic CO_2 responses (A-C_i) collected using a Li-6800 portable photosynthesis system during two field campaigns that took place during June and July 2019 (Cox et al., 2023) and during January and February 2022. The A-C_i data were measured under light-saturated conditions set at 1800 PPFD µmol photons m^{-2} s^{-1}, 60% relative humidity and by setting the block temperature of the Li-6800 to 29°C. Parameterisation of R_d was done using measurements of foliar respiration in the dark collected on the same leaves that A-C_i were measured, maintaining the same relative humidity and temperature as A-C_i data (Cox et al., 2023). A-C_i and R_d data were gathered from four individuals per species per site and were fed into the *Photosyn* function of the *plantecophys* R package (Duursma, 2015) to derive the photosynthetic parameters (apparent V_{cmax} and J_{max}) during each field campaign. Temperature response curves of apparent V_{cmax} and J_{max} were fitted with a modified Arrhenius equation (Medlyn et al. 2002) to estimate activation energy (E_a) and optimum temperature (T_{opt}), while fixing deactivation energy (H_d) at 200 kJ mol^{-1} (Dusenge et al. 2025). These kinetics were derived from A-C_i curves measured at five to six temperatures per site, ensuring that parameters reflected species-specific acclimation responses rather than default assumptions. We evaluated impact of accounting for acclimation of the temperature response of apparent V_{cmax} and J_{max} on model performance using the thermal acclimation equations from (Kumarathunge et al., 2019). Non-acclimated temperature responses parameters for apparent V_{cmax} and J_{max} were taken from Afromontane forests as described in Cox et al (2023).

We recognize that our parameter estimations are based on C_i rather than C_c, due to limitations in estimating mesophyll conductance. As a result, our estimates should be interpreted as apparent V_{cmax} and J_{max}. Measuring mesophyll conductance is particularly challenging under tropical field conditions and introduces uncertainty due to interspecific variation. Moreover, no standard model currently exists to represent the temperature sensitivity of mesophyll conductance. Therefore, as in many

studies (Dusenge et al., 2025), we used C_i-based parameterization for V_{cmax} and J_{max}, as well as for their acclimation models, which are useful for assessing temperature effects on photosynthesis in poorly studied tree species.

Diurnal cycles of net CO_2 assimilation (A_n) under ambient conditions were also collected using a Li-6800 portable photosynthesis system by taking spot measurements at different times of the day during two field campaigns. Measurements were performed on clear-sky days representative of typical climatic conditions at each site and within the same seasonal window to ensure comparability between locations. We measured three individuals per species, taking hourly measurements from 9:00 a.m. to 4:00 p.m. over three consecutive days. Before each measurement, the Li-6800 leaf chamber was opened to record ambient air temperature, relative humidity, and incoming radiation incident on each leaf. These environmental conditions were then imposed in the Li-6800 chamber, and leaves were enclosed under those same conditions. Data were recorded once gas exchange stabilized, which usually occurred within a few seconds. Diurnal cycles of An were measured on four individuals per species per site. A subset of the data (10%) was used to estimate the stomatal slope parameter (g_1) for each species and field campaign based on the Medlyn et al. (2011) model, as implemented in the *fitBB* function (*model option = "BBOpti"*) of the *plantecophys* R package (Lin et al., 2015; Duursma, 2015). The remaining data were divided for model calibration (65%) and evaluation (25%) (Figure 1).

Additionally, the following meteorological data from a Campbell weather station located at each experimental site were used in this study: air temperature (T_{air}, °C), relative humidity (that allow us estimate vapor pressure deficit (*VPD*, kPa)) and photosynthetic active radiation (*PAR*, µmol m^{-1} s^{-1}) recorded from January 2020 to June 2022 which included periods of physiological data collection.

2.4 Model parameterization and evaluation

A two-step approach was used to parameterize the model. First, species level average parameters (apparent V_{cmax}, apparent J_{max}, g_1, R_d) were used to run the model for each species at each site. To account for the observed intraspecific variability in our data sets (Cox et al., 2023) but also reported elsewhere in the Andes (Bahr et al., 2017;), the second approach uses the observed range of each parameter per species (i.e., the minimum, and maximum value in our dataset per each species) to select parameter combinations that improve model fitting. Here an iterative parameter selection procedure based on Monte Carlo Markov Chain (MCMC) methods was used: first, apparent V_{cmax} was randomly selected within the parameter's range for the target species, then the *Photosyn* function was run to evaluate whether model performance improved relative to the previous step. If model performance did not improve, the algorithm repeated this procedure ten times. The regression slope, the coefficient of determination (R^2), and the root mean squared error (RMSE) were used indicators of model performance. The expected slope of the linear model is one, the expected R^2 is also one, and zero for expected RMSE. If model performance improved, a new apparent V_{cmax} value close to the previous value got selected, the *Photosyn* function was rerun, and model performance was reassessed. This procedure was repeated 10000 times to find the apparent V_{cmax} parameter that best fitted the observations. After completing the search for apparent V_{cmax}, the same procedure was applied to apparent J_{max}, g_1, and R_d.

Parameter values from each iteration were used to calculate the probability distribution function of each parameter to represent the intraspecific variability that allows model fitting.

All simulations were performed with prescribed environmental drivers (*PAR*, T_{leaf}, *VPD*) as recorded by the Li-6800 during the A_n diurnal cycles and evaluated against the observed A_n. Model performance was assessed using a linear regression between the observed A_n from diurnal cycles and simulated using the *Photosyn* function by fixing the intercept of the linear model at zero. To evaluate model biases under different environmental conditions residuals of observed and simulated photosynthesis were plotted against C_i, *PAR*, T_{leaf}, *VPD*.

2.5 Sensitivity analysis

We evaluate the impact of intraspecific variability in photosynthetic traits on leaf level photosynthesis of tropical montane tree species comparing simulations from the two approaches used for model parameterization. The iterative approach allows to estimate a robust intraspecific distribution of physiological parameters for further interspecific comparisons.

To assess the relative contribution of physiological traits to diurnal variation of leaf level photosynthesis of tropical montane tree species at two thermal regimes (mean diurnal T_{air}, *VPD* and *PAR* during field campaigns for 14°C and 22°C sites), we used a Sobol index of variable importance which is particularly useful in complex models involving numerous inputs and nonlinear interactions. Sobol index is used to quantify the contribution and sensitivity of each input parameter (i.e. apparent V_{cmax}, apparent J_{max}, g_1, R_d) or the impact of their change to the output variance of a modelled variable (i.e A_n). The computation of Sobol index involves the creation of multiple model evaluations using systematically varied input values. Typically, a Monte Carlo method or other random sampling techniques are used to generate these evaluations. The indices are calculated based on the variance of model outputs due to the variance of each input. The equation for the first-order Sobol index is:

$$S_i = \frac{Var(E[Y|X_i)]}{Var(Y)} \quad (3)$$

Where, Y is the model output, X_i is the input parameter, and $E[Y|X_i]$ is the expected output under X_i parameter.

Here Sobol indices are used to assess the effect of varying apparent V_{cmax}, apparent J_{max}, g_1 and R_d, within their measured distributions in our data set, on simulated A_n under different environmental conditions throughout the diurnal cycle. For this sensitivity analysis, the photosynthesis model was applied using average 30-minute weather station data recorded during the period that the measurements of diurnal cycles of A_{net} took place. Subsequently, a matrix containing 10,000 different values for each parameter, consistent with the distributions obtained from our iterative search approach (as previously described in Model paremeterisation and evaluation section) was constructed. The *sobol_indices* function from the *sensobol* R package (Puy et al., 2022) was used to calculate the Sobol indices.

To assess the relative contribution of key environmental drivers of photosynthesis (T_{air}, *VPD* and *PAR*) in tropical montane tree species we also make use of the Sobol index. The computation of the Sobol index requires fixing some values while iterating over the target variable or parameter, in this case, the environmental variables. Therefore, we held the physiological

parameters at known values representing the observed variation of these parameters in the studied species as follows. We used observed minimum, average, and maximum values of g_1 (2.5, 5 and 7.5 $kPa^{0.5}$) and the J_{max}: V_{cmax} ratio (1.75, 2.5 and 3) that represent both, montane and lowland species, and the full range of observed variations in V_{cmax} (25 to 75 µmol m^{-2} s^{-1}). Subsequently, we used T_{air}, *VPD* and *PAR* from the weather station at each site to define the range of each variable and constructed a matrix with 10,000 values per variable and then ran the Sobol index analysis.

2.6 Model application

To evaluate whether the common assumption in large-scale models—using mean photosynthetic parameters derived from lowland species to simulate montane forest photosynthesis—is a valid approach, we compared simulations including both montane and lowland tree species with those including only lowland species under identical environmental conditions. Photosynthesis was simulated using best-fit parameter values for montane and lowland species at each site, together with one year of hourly weather station data from the 14 °C and 22 °C sites. The relative abundances of montane and lowland species used in the simulations were based on field observations reported in previous studies of tropical Andean forests (Duque et al., 2015; González-Caro et al., 2020). Montane species represent approximately 75% of the total species above 2200 m a.s.l. (14 °C site) and about 30% between 1200–2000 m a.s.l. (22 °C site). Accordingly, we simulated forests with these respective proportions of montane and lowland species to reflect realistic community composition. The simulations aimed to assess how the magnitude and temporal stability of average photosynthesis change depending on whether one or both plant functional groups are considered. We simulated leaf-level photosynthesis for one year at each site under both scenarios (only lowland vs. lowland + montane species). Monthly totals were obtained by summing daily values, and scenarios were compared using paired *t*-tests. Finally, we calculated the percentage change in photosynthesis between scenarios to quantify the influence of including montane species in model parameterisation.

3. Results

3.1 Overall FvCB model performance

We modelled photosynthesis with the *FvCB* model for eight tree species, comprising six montane species and two lowland species from the tropical Andes. Inclusion of thermal acclimation of the temperature response of photosynthetic capacity improved model performance by ~ 20% (Table 1). Using the best approaches to select model parameters based in our analyses (iterative searching for physiological parameters) and thermal acclimation of the temperature response of photosynthetic capacity, model fitting showed high model performance (averaged $R^2 = 0.90$; Figure 2a), suggesting that the model with best fit parameters accurately simulate photosynthesis for these species when accounting for intraspecific variation (Figure S1, Table 1). Overall, simulated A_n represents the observed diurnal variation with high accuracy (Table 1), although there model tends to underpredict the observations at very high *PAR* or T_{air} at the 14°C site and over predict at high *VPD* at the 22°C site

(Figure S2). Model performance was best for all species at sites close to their native environments: specifically, species level model application for montane species was closest to observations at the 14°C site and similarly for lowland species at the 22°C (Table 1). The model application for montane species also showed very good performance under warming (i.e., 22°C site), with the main model observational biases happening around noon (1200–1400 hours, Figure S2) with a slight trend to overestimate the observations (β >1 in Table 1). In contrast, model application for lowland species under the cold environment (i.e., 14°C site,) showed intermediate values of model performance (*Inga marginata*, $R^2 = 0.58$ and *Inga spectabilis*, $R^2 = 0.61$) and also exhibited a significant reduction in simulated A_n respect to simulations at the 22°C site (Table 1; β = 0.81 and β=0.83, respectively).

3.2 Intraspecific variability effect on model performance

Model performance improved across all species and sites when using the iterative parameter searching approach (R^2= 0.90, RMSE = 0.20, β = 1.09) compared to simulations that relied on average parameter values (R^2= 0.78, RMSE = 0.52, β = 0.91). This suggest that intraspecific variation of physiological traits plays a crucial role in enhancing model accuracy and reducing prediction errors (Table 1 and 2). Specifically, apparent V_{cmax} values obtained from the iterative searching method were, on averaged, 1.4 times higher than species-level mean values (Figure 2b), emphasizing the importance of capturing trait variability rather than relying solely on species-level means. Similarly, the stomatal conductance parameter g_1 also showed a variation in the selected value via iterative searching compared to the average observed value and the former tended to be highest, but their shift was no systematic (Figure 2d). In contrast, the effect of apparent J_{max} (Figure 2c) and R_d in model calibration was negligible (plots for R_d not shown), indicating that not all physiological parameters contribute equally to model performance improvements.

3.3 Contribution of physiological traits to diurnal variation of simulated photosynthesis

Apparent V_{cmax} was found to have the largest relative contribution to diurnal variation in simulated leaf level photosynthesis in all cases, accounting for ~56% (averaged throughout the day for all groups and sites, Figure 3). The relative contribution of apparent V_{cmax} is lower at the native environment for montane (~52%) and lowland (~41%) species than at at 22°C (~61%) or 14°C (~65%) environments, respectively (Figure 3). Specifically, at 14°C, there were larger contributions from apparent J_{max} to A_{net} in montane (17.2 %) than in lowland (9.5%) species. And at 22°C, lowland species had larger contribution from apparent J_{max} (16.1%) than montane species (5.7%). Also, at 22°C, g_1 had the second largest contribution to A_n for both groups of species (Figure 3 c,d) (13.6% montane and 16.8% for lowland) with importance increasing in the afternoon in response to high leaf to air vapor pressure deficit. Respective g_1 contributions to A_{net} at 14°C were 6.5% for montane and 6.2% for lowland species

(Figure 3 a,b). The contribution of R_d and interactions among parameters were low (~4%) and similar across species groups and sites throughout the day (Figure 3).

3.4 Impact of environmental conditions on leaf photosynthesis of tropical montane species

We found differences in the influence of environmental variables (T_{air}, *VPD* and *PAR*) on simulated A_n between both sites, 14°C (Figure 4) and 22°C (Figure 5). Overall, at 14°C *PAR* and T_{air} are the main drivers of A_n with contributions of 48% and 39% respectively (values averaged across comparisons; Figure 4). At 22°, *VPD* and T_{air} are the main drivers of A_n with a contribution of 37% and 28% (averaged across comparisons; Figure 5). In sum, the relative contributions of *PAR* and T_{air} to A_n are larger at 14°C than at 22°C and vice versa for *VPD.*

Specifically, at the 14°C site, for the range of studied values of J_{max}: V_{cmax} for both montane and lowland species, photosynthesis is primarily controlled by temperature and *PAR* (Figure 4), and their relative contributions are mediated by g_1 (i.e., stomatal conductance). When g_1 is close to 2.5, meaning a conservative plant water use strategy, the relative importance of *VPD* increases with decreasing apparent V_{cmax} (Figure 4 a,b,c), whereas under g_1 values above 2.5 (more wasteful water use strategy), air temperature increases its relative importance (Figure 4 d,e,f). Under high g_1 values, *PAR* has a large contribution to photosynthesis at low J_{max}: V_{cmax} and the relative importance of T_{air} increases with increasing J_{max}: V_{cmax} (Figure 4 g,h,i). On the other hand, at the 22°C site, photosynthesis is primarily controlled by *VPD* under low g_1 values (2.5), independently of J_{max}: V_{cmax} (Figure 5 a,b,c). When, g_1 increases, the influence of *VPD* decreases while the contribution of T_{air} increases (Figure 5 d,e,f). Additionally, under low J_{max}: V_{cmax} values, the relative contribution of *PAR* increases (Figure 5 d,g).

3.5 Relative contribution of montane and lowland species to average photosynthesis

We found large differences between simulations that included both montane and lowland species and those based solely on lowland species. At the 14°C site, simulations incorporating both groups produced larger annual photosynthesis than including solely lowland species (t = -4.65; P < 0.001 Figure 6a). On average, 65% higher photosynthesis during at least six months of the year compared to simulations using only lowland species parameters. This period coincided with lower solar radiation levels. Conversely, during months with higher solar radiation and reduced cloud cover, simulations including both groups yielded ~25% lower photosynthesis than those using only lowland species (Figure 6a). In contrast, at the 22°C site, simulations using only lowland species consistently resulted in 29% higher photosynthesis, on average, across the entire year compared to simulations including both species groups (Figure 6b).

4. Discussion

4.1 Intraspecific variability of photosynthetic traits

Our results display large variability in photosynthetic traits of montane tree species. This ranges from species with higher photosynthesis capacity like *Miconia theizans* (apparent V_{cmax} = 135 mmol m^{-2} $s^{-1}$and apparent J_{max}= 210 mmol m^{-2} s^{-1}) to *Quercus humboldtii* (apparent V_{cmax} = 65 mmol m^{-2} s^{-1} and apparent J_{max}= 115 mmol m^{-2} s^{-1}; Figure S1). The high interspecific variance in photosynthesis traits could stem from their ecological origin, environmental heterogeneity and phylogenetic position (Yan et al., 2023). This variance can influence the community-level response of tropical Andean forests to climate. If photosynthesis traits, such as apparent V_{cmax} or J_{max}, of a single species are negatively impacted by high temperature, low humidity, or low light availability, a different species may compensate and maintain ecosystem functioning. For example, under environmental conditions similar to the 14°C site, which is the site closest to the optimal temperature conditions to which many tropical montane species are adapted to, *Miconia theizans* and *Clusia multiflora* exhibit high photosynthetic capacity (apparent V_{cmax}) but, because of their low water use efficiency (g_1), are strongly affected by the warmer and drier conditions experienced at the 22°C site (Figure S1), which is at the warm extreme of the thermal range of these species. In contrast, *Quercus humboldtii*, maintains a similar photosynthetic capacity (apparent V_{cmax}) at both sites, suggesting that the Andean oak is more tolerant to warming and can help tropical Andean forests be resilient to climate change. Therefore, the combination of species with different photosynthesis traits may positively influence productivity, as high interspecific variance can help maintain stable levels across a wide range of environmental conditions, including variations in air temperature, VPD or solar radiation. Here, we suggest that regional predictions of photosynthesis and carbon dynamics of tropical Andean forests should include interspecific variation in photosynthetic traits and how particular combinations of these traits maintain high photosynthesis rates under changing environmental conditions (Bahar et al., 2017), Figure 6e).

Surprisingly, intraspecific and interspecific variance of the physiological traits in our data set are of similar magnitudes (σ^2 intra = 28% to σ^2 inter = 43% of total variance). Our parametrization approach, which iteratively searches for the combination of physiological traits (apparent V_{cmax}, apparent J_{max} and g_1), improves prediction of photosynthetic rates. The large difference between the best fitted physiological trait values relative to average observed values suggest that every leaf/tree adjusts their physiology to the experienced environmental conditions to maintain photosynthesis. Therefore, our analysis highlights the importance of field-based measurements and the inclusion of intraspecific variance in physiological traits to be used in vegetation modelling (Maréchaux et al., 2024). Given this variability, an important question arises: how does trait variation influence overall canopy functioning metrics? If trait variability is not explicitly considered, do we risk misrepresenting canopy-level photosynthetic performance? The ability of species to rapidly acclimate to changing conditions suggests a potential compensatory mechanism, but it remains unclear whether this plasticity is sufficient to maintain overall canopy function at similar levels or if significant differences emerge under shifting environmental conditions. Addressing this uncertainty is crucial for refining dynamic vegetation models, as compensatory responses could either buffer or amplify ecosystem-level responses to climate change. The high variability of photosynthetic traits and the ability of species to acclimate

to changing conditions may be adaptations to the high environmental variability that occurs in montane forests (Fyllas et al., 2017). Furthermore, intraspecific variance can enhance interspecific variance in terms of maintaining photosynthesis under increased warming (Bassow and Bazzaz, 1997; Zaka et al., 2016). Therefore, the explicit inclusion of intra- and interspecific variance in dynamic vegetation models can improve our ability to understand the response of tropical montane forests to future warming.

We found that the stomatal conductance trait (g_1) showed the highest intraspecific variance detected by our approach, suggesting that stomatal control is critical to maintaining photosynthesis under changing environmental conditions. The intraspecific variance of functional traits has been highlighted as an overlooked diversity property that can influence the community response to environmental conditions (Lin et al., 2015). For example, the intraspecific variance of leaf morphological traits such as leaf mass per area has been globally evaluated, showing that intra- and interspecific variance can be similar in magnitude (Anderegg et al., 2018; Siefert et al., 2015). This result aligns with our findings on physiological traits in montane tropical forest; however, measuring intraspecific variance for physiological traits is more challenging due to logistical constraints and the time-consuming measurements that are needed. Our approach, which combines diurnal cycle measurements of photosynthesis that can be easily taken in the field with computational and modelling methods, can help describe the intraspecific variance of tropical montane species.

4.2 Contribution of physiological traits to diurnal variation of leaf photosynthesis

Our results indicate that apparent V_{cmax} plays a dominant role in regulating photosynthesis (A_n) in both montane and lowland tree species, contributing approximately 56% of simulated A_n. The contribution of apparent V_{cmax} increases when species are subjected to temperature changes (warming for montane species and cooling for lowland species), suggesting that carboxylation capacity is a key driver of Andean Forest responses to climate change. Conversely, apparent J_{max} plays a more significant role in regulating A_n in species growing in their native environments, implying that its influence is linked to local environmental conditions. This raises an important question: will photosynthetic responses to increased temperatures under future climate be primarily driven by apparent V_{cmax} as our results suggest, or could apparent J_{max} regain dominance through acclimation processes? The fact that apparent J_{max} is strongly coupled to the light environment in both montane and lowland species suggests that changes in light availability could modulate its role in photosynthetic regulation (Fyllas et al., 2017). Montane trees, which naturally experience low and fluctuating light conditions, may be more constrained by light interception traits, whereas lowland species, adapted to more stable but lower-intensity light conditions, might rely on different acclimation strategies (Marthews et al., 2012). Therefore, while leaf traits related to light interception appear crucial for in situ performance, their significance under climate warming remains uncertain. If temperature increases lead to shifts in light availability (e.g., through cloud displacement or canopy restructuring), species with traits optimizing light capture could gain a competitive advantage. However, further research is needed to determine whether light interception remains a limiting factor under warming or if apparent V_{cmax} -driven biochemical responses will dominate photosynthetic acclimation.

The relative contribution of simulated stomatal conductance (g_1) increases in the afternoon, mainly at the 22°C site, in which T_{air} and *VPD* commonly increase with respect to the 14°C site. This is likely a response to high leaf-to-air vapor pressure deficit, indicating that a rapid stomatal response (g_1) is crucial for regulating water loss and gas exchange under conditions of high *VPD*, helping maintain photosynthetic efficiency and preventing excessive water loss. The high variability of g_1 detected by our parametrization approach indicates that the species with high stomatal control ability can persist under the high environmental heterogeneity imposed by tropical highland conditions (Guo et al., 2022). Here, we suggest that the dynamic role of g_1 in response to *VPD* should also be incorporated into models to better predict diurnal and seasonal photosynthetic performance and the differential responses of montane and lowland species to temperature and *VPD* highlighting the importance of biodiversity in maintaining ecosystem function (Smith et al., 2020).

4.3 Environmental influence on photosynthesis in the tropical highlands

We found differences in the role of environmental drivers on simulated leaf level photosynthesis at the two study sites, 14°C (2500 m a.s.l.) and 22°C (1400 m a.s.l.) (Figure 4 & Figure 5). At the 14°C site, Photosynthetically Active Radiation (*PAR*) and air temperature (T_{air}) have a stronger influence on simulated photosynthesis, whereas at the 22°C site, atmospheric demand (*VPD*) plays a more dominant role. This suggests that, at higher elevations, where temperatures are low and *VPD* is naturally reduced, radiation becomes the primary climatic driver of photosynthesis. Since T_{air} partly determines *VPD*, its lower influence at 14°C may explain why *PAR* exerts a stronger control on simulated photosynthesis at this site. Tropical montane forests frequently experience low and fluctuating solar radiation due to persistent cloud cover and fog, leading to the adaptation of montane tree species to these conditions (Fyllas et al., 2017). In contrast, lowland species, which are beginning to colonize higher elevations, may compensate for the reduced and variable light by increasing their photosynthetic capacity, primarily through higher apparent V_{cmax} values (Bahar et al., 2017; Yan et al., 2023). This raises an important question: how does temperature interact with radiation limitation across different thermal environments? While our findings suggest that PAR limits photosynthesis at high elevations (low T_{air}), it is also possible that radiation constrains photosynthesis at high temperatures, particularly if warming leads to increased cloud displacement along mountain slopes. If climate change results in increased solar radiation at higher elevations, this could raise leaf temperatures, negatively affecting montane species adapted to cooler conditions while favoring thermophilisation—the upward migration of lowland species (Duque et al., 2015; Fadrique et al., 2018; Cuni-Sanchez et al., 2024).

Our analyses suggest a key role for stomatal conductance (g_1), a highly inter and intraspecific variable trait, in mediating the effects of *PAR*, *VPD*, and T_{air} on the diurnal variation of simulated An. Under low values of g1, photosynthesis is mainly influenced by T_{air} and *VPD* at both sites. However, the effect of T_{air} is larger at 14°C, while *VPD* has a stronger effect at 22°C. This suggests that under low stomatal conductance, photosynthesis at high elevations (14°C site at 2500m a.s.l.) is primarily constrained by biochemical limitations due to low temperatures, whereas at intermediate elevations (22°C site at 1400m a.s.l.),

stomatal control dominates through the indirect effect of Tair on *VPD*. A key mechanism driving these differences may be the role of apparent V_{cmax} in controlling gross primary productivity (*GPP*) responses to temperature (Marthews et al, 2012). At low Tair, biochemical limitations require a higher apparent V_{cmax} to sustain high *GPP*, as enzymatic reactions slow down at colder temperatures. If apparent V_{cmax} does not scale accordingly, *GPP* remains limited by temperature (Marthews et al, 2012). However, maintaining high apparent V_{cmax} is metabolically costly, meaning some montane species may instead favor a strategy of lower apparent V_{cmax} combined with rapid stomatal responses to optimize carbon gain and water use efficiency. Conversely, under warming conditions, apparent V_{cmax} appears less responsive to temperature than apparent J_{max}, suggesting that lack of apparent V_{cmax} acclimation could negatively impact GPP. While J_{max} can respond dynamically to increased temperatures, a relatively unacclimated apparent V_{cmax} may impose a biochemical bottleneck, further limiting photosynthetic potential under future warming (Marthews et al., 2012). This introduces two critical processes: i) The need for a higher apparent V_{cmax} at low temperatures to compensate for temperature-related biochemical constraints on *GPP*, balanced against the metabolic costs of maintaining such high enzymatic activity. ii) The lower responsiveness of apparent V_{cmax} compared to apparent J_{max} under warming, which may restrict acclimation potential, making tropical montane species increasingly vulnerable to climate change (Smith et al., 2020). These findings reinforce the necessity of incorporating thermal acclimation of temperature-dependent responses of both apparent V_{cmax} and apparent J_{max} into models predicting future forest productivity under climate change.

On the other hand, when apparent V_{cmax} and apparent J_{max} are high (under all g_1 cases tested), photosynthesis is primarily controlled by *PAR* and the influence of *VPD* is significantly reduced with increasing g_1. This suggest that high g_1 species with high photosynthetic capacity are less constrained by *VPD* and temperature, with *PAR* being the dominant factor. This indicates that species with higher photosynthetic capacities can better exploit available light for photosynthesis, reducing their sensitivity to other environmental stressors. Montane and lowland species have evolved different mechanisms to optimize photosynthesis, reflecting their adaptation to their unique environments. For lowland species, maximising photosynthesis capacity could be an advantageous strategy. However, this strategy is unstable on tropical highlands because of the fluctuating nature of light conditions, due to frequent fog and cloudiness. Therefore, a more favourable, i.e. resource-efficient, photosynthesis strategy under these conditions can be low apparent V_{cmax} combined to high stomatal control for rapid response to changing conditions (Bahar et al., 2017; van de Weg et al., 2012). This highlights the importance of understanding the physiological and anatomical features that determine the ability to control stomatal conductance (g_1) response under stressful conditions such as tropical mountains for maintaining photosynthesis.

4.4. Recommendations for photosynthesis modelling in montane forests

We found that total photosynthesis in montane forests is related to local conditions (e.g., elevational and climate) but also to species composition at each site (montane and lowland species). Although, we expected the contribution of montane species to be larger at 14°C and vice versa for lowland species at 22°C, we found that combining the parametrization of both species

groups increases the photosynthesis estimation of montane forests and a reduction in lowlands (Bahar et al., 2017; Cox et al., 2023; Dusenge et al., 2025). High-elevation conditions can be adverse for lowland species, and their modelled photosynthetic responses likely underestimate actual forest productivity at these sites. This may lead to a misinterpretation of the effects of low solar radiation and persistent cloud cover, as montane tree species tend to perform better under such conditions. Conversely, photosynthesis in lowland forests between 1000 and 1800 m a.s.l. may be overestimated in models that do not account for the presence of montane species. This result highlights the importance of accounting for community composition (e.g., proportion of montane vs lowland with their corresponding parameters) to model photosynthesis at landscape scale. Common large modelling approaches are restricted to use mean values of physiological parameters and exclude the high observed species level variability. Also, the differential response of each species group to environmental conditions needs to be accounted for in large scale modelling because the response of species to T_{air}, *VPD* and *PAR* varies along elevation and by species adaptations to their origin climates (Yan et al., 2023). Our results demonstrate large variability in g_1 and suggest that it is important to incorporate this high variability when modelling stomatal conductance under the heterogeneous environmental conditions of tropical elevational gradients. In sum, we recommend using specific parameterisations for montane and lowland species when modelling montane forest and caution for modelling approaches with respect to using invariant physiological parameters when modelling along complex environmental gradients such as in tropical montane forests as this can obscure photosynthesis response to rapidly changing conditions. However, our findings are based on juvenile trees growing without competition and thus should be interpreted as reflecting potential physiological responses rather than realised ecosystem-scale productivity. Nevertheless, because juveniles often exhibit higher photosynthetic capacity and represent the future cohorts of these forests, they provide valuable insights into the mechanisms that will likely shape mature forest responses to ongoing warming.

Table 1. Photosynthesis model performance for all study species applied at two experimental sites (14°C and 22°C) using three indicators: Regression slope between observed and predicted values (β), residual mean squared error (RMSE) of final model, and coefficient of determination (R^2) at individual-level parametrization (iterative modelling approach) plus acclimation (ind + acclim), species level parametrization plus acclimation (sp + acclim) and species level parametrization without acclimation (sp). Species were separated in two groups (montane and lowland) accordingly to their thermal affiliation and elevational distribution.

Group	Species	Site	β	RMSE	R^2 (ind + acclim)	R^2 (sp + acclim)	R^2 (sp)
Montane	*Clusia multiflora*	14°C	1.07	0.14	0.91	0.77	0.61
Montane	*Clusia multiflora*	22°C	1.12	0.23	0.83	0.62	0.52
Montane	*Miconia theizans*	14°C	0.97	0.14	0.94	0.71	0.59
Montane	*Miconia theizans*	22°C	1.23	0.26	0.82	0.69	0.55
Montane	*Quercus humboldtii*	14°C	0.99	0.04	0.97	0.78	0.56
Montane	*Quercus humboldtii*	22°C	1.05	0.19	0.89	0.75	0.61
Montane	*Andesanthus lepidotus*	14°C	0.97	0.21	0.93	0.76	0.57
Montane	*Andesanthus lepidotus*	22°C	1.21	0.34	0.80	0.74	0.52
Montane	*Clethra fagifolia*	14°C	1.05	0.16	0.94	0.77	0.61
Montane	*Clethra fagifolia*	22°C	1.17	0.29	0.79	0.68	0.57
Montane	*Weinmmania pubescens*	14°C	1.03	0.15	0.93	0.73	0.55
Montane	*Weinmmania pubescens*	22°C	1.32	0.26	0.81	0.69	0.52
Lowland	*Inga marginata*	14°C	0.83	0.91	0.58	0.52	0.43
Lowland	*Inga marginata*	22°C	0.97	0.17	0.93	0.74	0.58
Lowland	*Inga spectabilis*	14°C	0.81	0.82	0.61	0.50	0.41
Lowland	*Inga spectabilis*	22°C	1.02	0.18	0.91	0.69	0.49

Table 2. Photosynthetic parameters (*Vcmax* and *Jmax* in µmol m^{-2} s^{-1}, and their ratio *Jmax : Vcmax*) expressed as maximum (max), minimum (min), and mean (mean) values for montane and lowland species at each site (14 °C and 22 °C) used for sensitivity analyses. The maximum and minimum values represent the absolute range of fitted parameters across all individual observations for each species group.

	Montane		Lowland	
	14 °C	22 °C	14 °C	22 °C
V_{cmax} min	50.01	29.68	23.43	32.94
V_{cmax} mean	77.59	46.99	34.70	56.42
V_{cmax} max	120.58	73.66	45.23	72.56
J_{max} min	129.48	80.24	74.35	83.08
J_{max} mean	180.07	127.90	100.04	122.70

	2 1 1 1
	5 9 1 5
	0. 0. 9. 2.
	8 1 5 4
J_{max} max	1 9 4 9
	2. 2. 2. 2.
	0 1 5 0
J_{max} : V_{cmax} min	1 5 6 1
	2. 2. 2. 2.
	4 7 9 3
J_{max} : V_{cmax} mean	8 2 4 6
	2. 3. 3. 2.
	9 2 3 7
J_{max} : V_{cmax} max	7 9 3 4

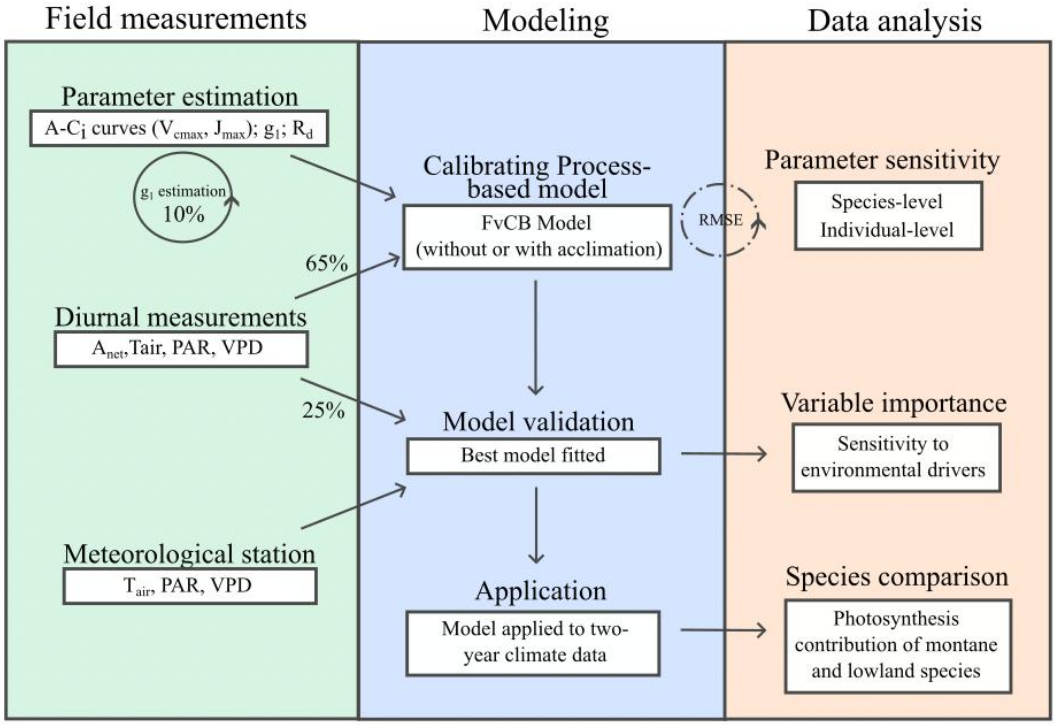

Figure 1. Summary of methodology applied in this study comprising field measurements, modelling (calibration and evaluation) and data analysis related to sensitivity analyses.

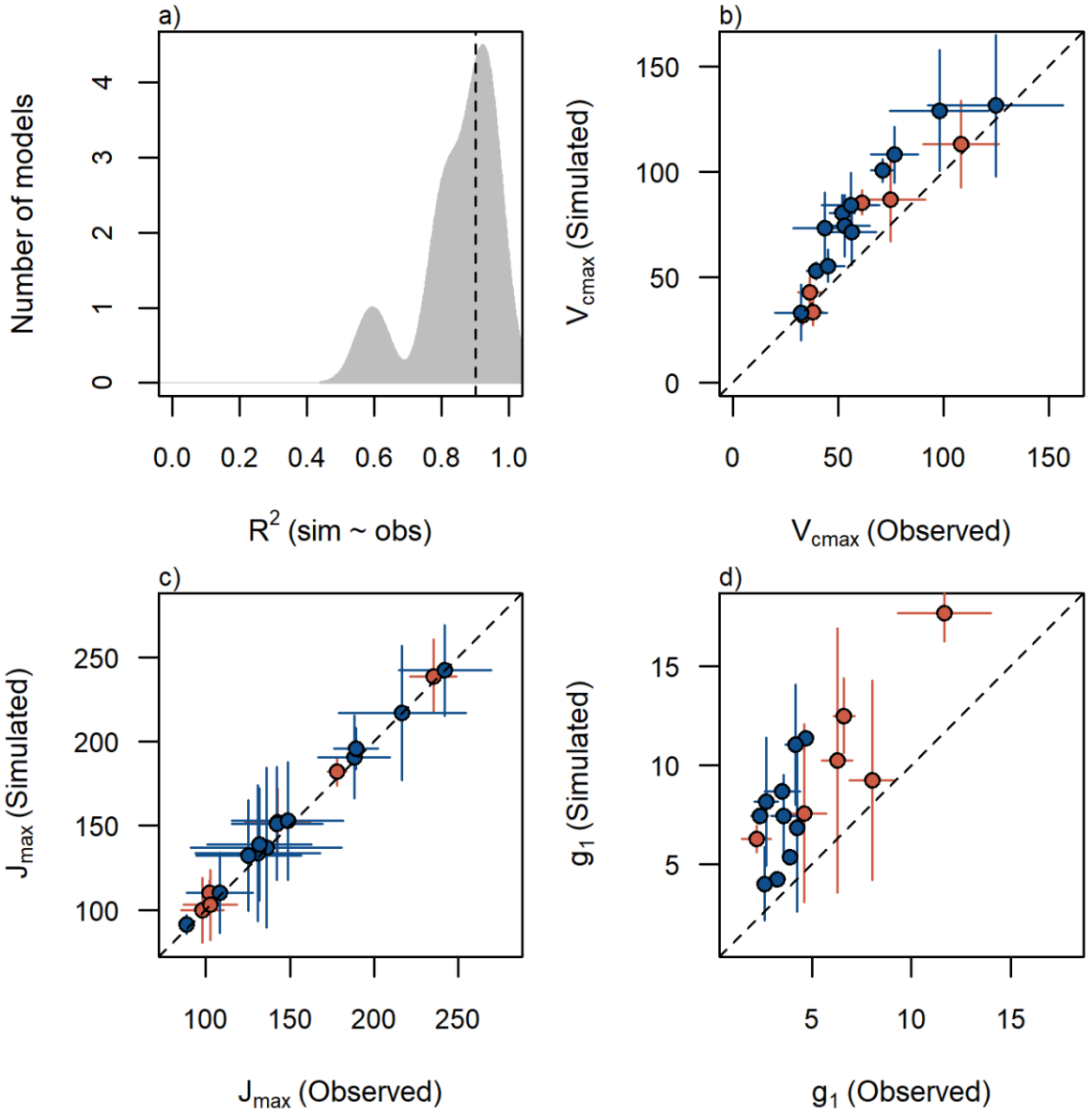

525

Figure 2. Model performance using the iterative parameter searching approach. (a) R^2 distribution of final best model parameterization per species per site for all species and sites. The dashed line represents the median. Relationship between observed average parameter value and predicted value by the iterative searching approach for (b) V_{cmax} (μmol m^{-2} s^{-1}), (c) J_{max} (μmol m^{-2} s^{-1}) and (d) g_1 ($kPa^{0.5}$) per species per site. Blue circles represent montane species, and red circles are lowland species. Error bars are 530 **added to each point representing standard error of observed values in y-axis and range of simulated values in x-axis. Dashed lines indicate the 1:1 relationship.**

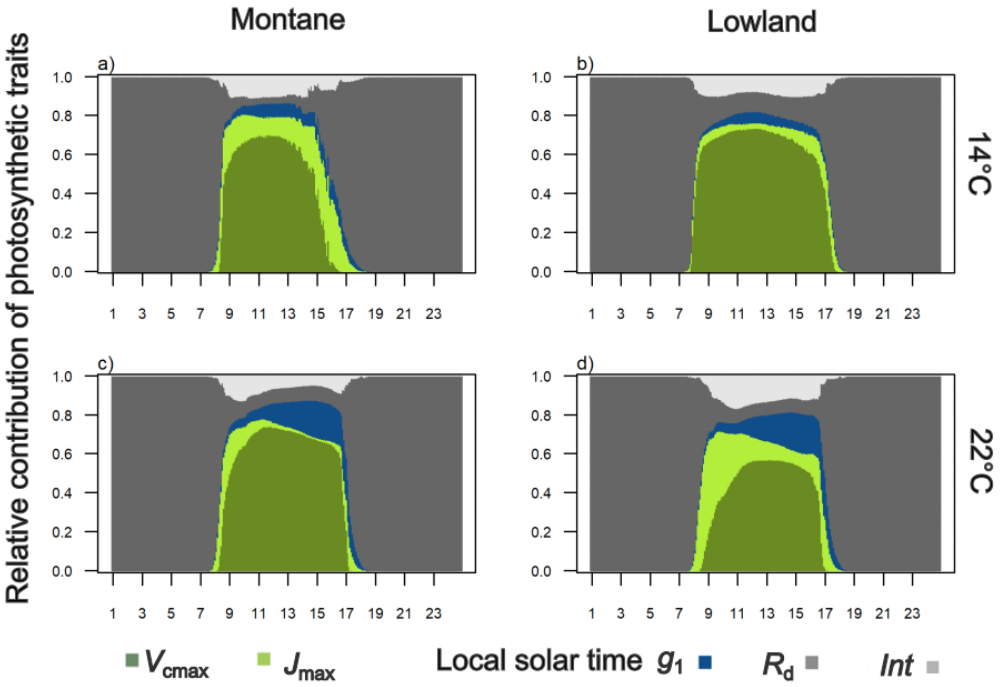

Figure 3. Diel variation of the simulated relative contribution of physiological parameters to simulated leaf-level net carbon uptake for montane (a and c) and lowland species (b and d), at two growth temperatures (14°C and 22°C). Light grey represents interaction (*Int*) among study parameters.

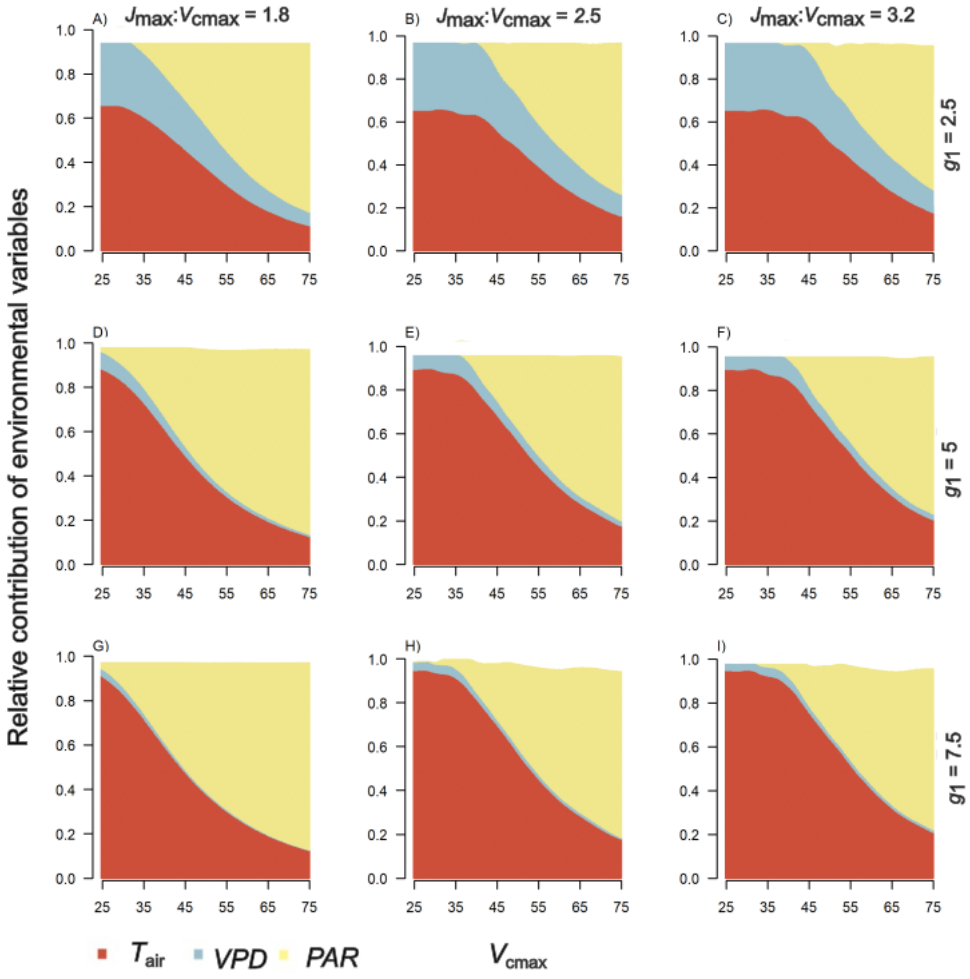

Figure 4. Simulated relative contribution of environmental conditions (T_{air} [14-25 °C], *VPD* [0.6-2.4 kPa] and *PAR* [200-1600 µmol m^{-2} s^{-1}]) to leaf level net photosynthetic uptake at the 14°C site. The x-axis is the V_{cmax} (µmol m^{-2} s^{-1}) range of most common values of this parameter in field data. Panel columns represent different values of the ratio between J_{max} (µmol m^{-2} s^{-1}) and V_{cmax} (µmol m^{-2} s^{-1}) observed in field data (Table 2). Panel rows represent different g_1 ($kPa^{0.5}$) values observed in montane and lowland species.

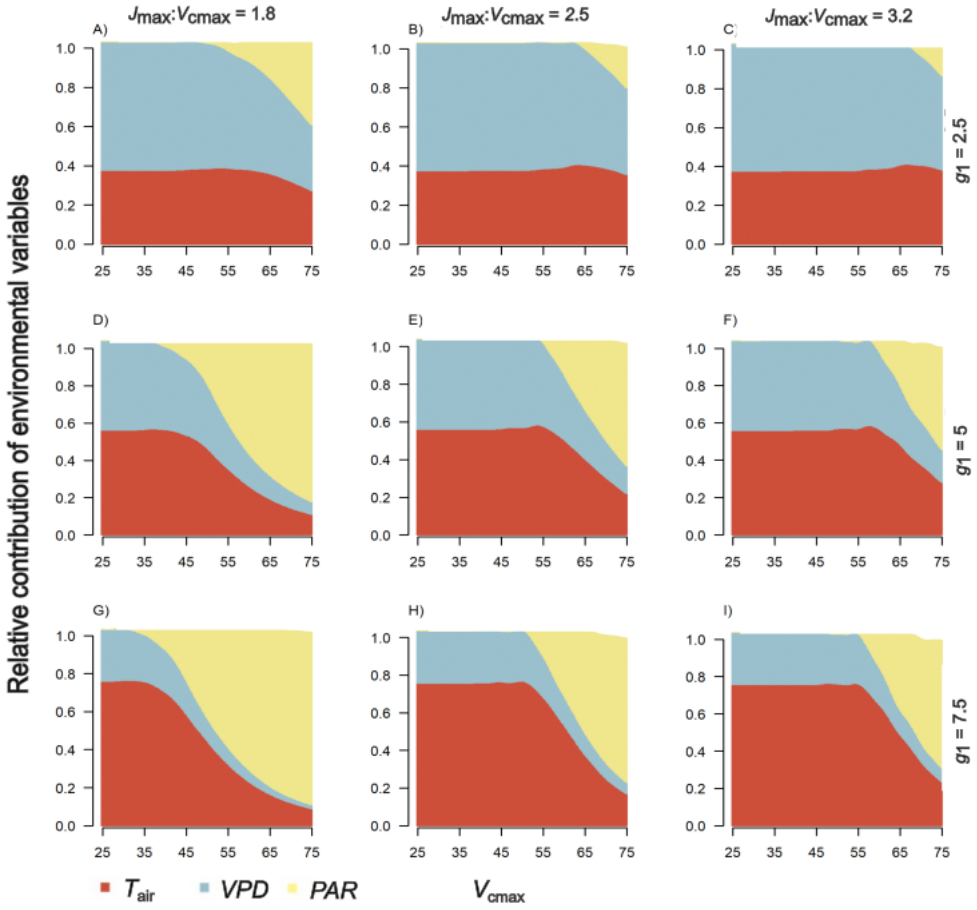

Figure 5. Simulated relative contribution of environmental conditions (T_{air} [19-35 °C], *VPD* [1-3.8 kPa] and *PAR* [400-1600 µmol m^{-2} s^{-1}]) to the 22°C site to leaf level net photosynthetic uptake. The x-axis is the V_{cmax} (µmol m^{-2} s^{-1}) range of most common values of this parameter in field data. Panel columns represent different values of the ratio between J_{max} (µmol m^{-2} s^{-1}) and V_{cmax} (µmol m^{-2} s^{-1}) observed in field data (Table 2). Panel rows represent different g_1 (kPa$^{0.5}$) values observed in montane and lowland species.

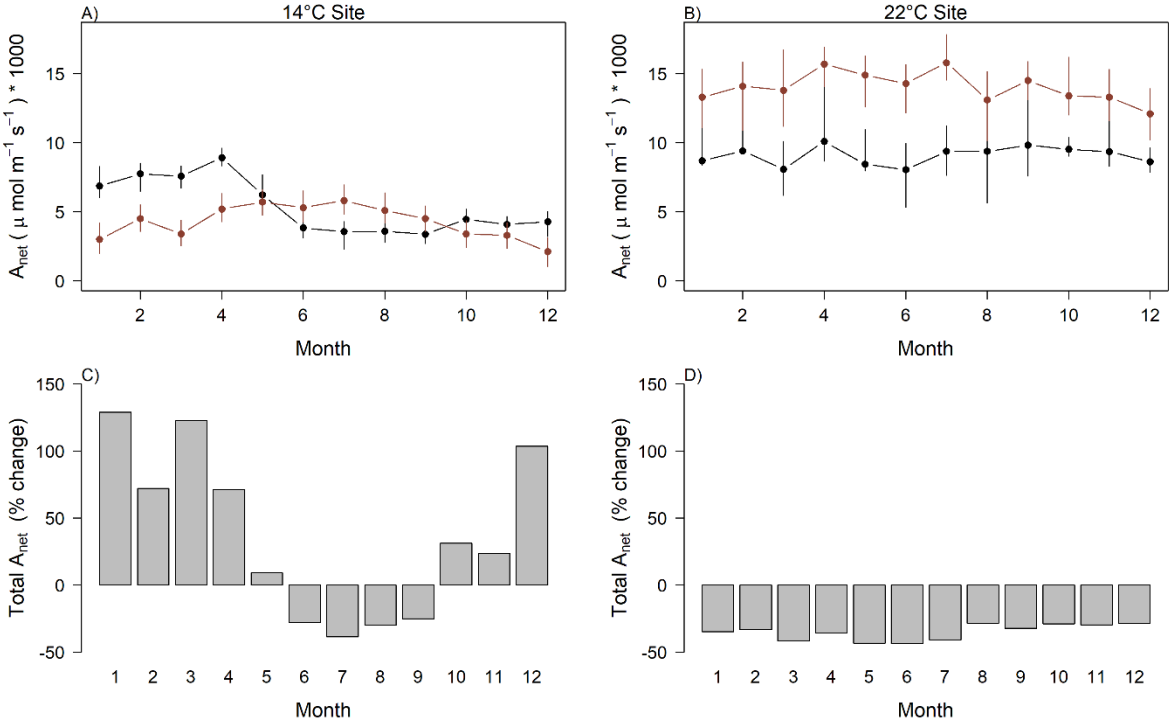

Figure 6. Simulated leaf level photosynthesis (A_{net} (µmol m^{-2} s^{-1})) including montane and lowland species weighing their contribution accordingly to their abundance in a forest of 1000 individuals (black) and only lowland species assuming all individuals correspond to this group (red) under environmental conditions at the (a) 14°C site and at the (b) 22°C site. Percentage change in the photosynthesis including both species groups (montane and lowland) relative to only include lowland species for each site, respectively (c, d).

References

Anderegg, L. D. L., Berner, L. T., Badgley, G., Sethi, M. L., Law, B. E., and HilleRisLambers, J.: Within-species patterns challenge our understanding of the leaf economics spectrum, Ecology Letters, 21, 734–744, https://doi.org/10.1111/ele.12945, 2018.

Bahar, N. H. A., Ishida, F. Y., Weerasinghe, L. K., Guerrieri, R., O'Sullivan, O. S., Bloomfield, K. J., Asner, G. P., Martin, R. E., Lloyd, J., Malhi, Y., Phillips, O. L., Meir, P., Salinas, N., Cosio, E. G., Domingues, T. F., Quesada, C. A., Sinca, F., Escudero Vega, A., Zuloaga Ccorimanya, P. P., del Aguila-Pasquel, J., Quispe Huaypar, K., Cuba Torres, I., Butrón Loayza, R., Pelaez Tapia, Y., Huaman Ovalle, J., Long, B. M., Evans, J. R., and Atkin, O. K.: Leaf-level photosynthetic capacity in lowland Amazonian and high-elevation Andean tropical moist forests of Peru, New Phytologist, 214, 1002–1018, https://doi.org/10.1111/nph.14079, 2017.

Bassow, S. L. and Bazzaz, F. A.: Intra- and inter-specific variation in canopy photosynthesis in a mixed deciduous forest, Oecologia, 109, 507–515, https://doi.org/10.1007/s004420050111, 1997.

Cox, A. J. F., Hartley, I. P., Meir, P., Sitch, S., Dusenge, M. E., Restrepo, Z., González-Caro, S., Villegas, J. C., Uddling, J., and Mercado, L. M.: Acclimation of photosynthetic capacity and foliar respiration in Andean tree species to temperature change, New Phytologist, 238, 2329–2344, https://doi.org/10.1111/nph.18900, 2023.

Cox, A. J. F., González-Caro, S., Meir, P., Hartley, I. P., Restrepo, Z., Villegas, J. C., Sanchez, A., and Mercado, L. M.: Variable thermal plasticity of leaf functional traits in Andean tropical montane forests, Plant Cell and Environment, 47, 731–750, https://doi.org/10.1111/pce.14778, 2024.

Cuni-Sanchez, A., Sullivan, M. J. P., Platts, P. J., Lewis, S. L., Marchant, R., Imani, G., Hubau, W., Abiem, I., Adhikari, H., Albrecht, T., Altman, J., Amani, C., Aneseyee, A. B., Avitabile, V., Banin, L., Batumike, R., Bauters, M., Beeckman, H., Begne, S. K., Bennett, A. C., Bitariho, R., Boeckx, P., Bogaert, J., Bräuning, A., Bulonvu, F., Burgess, N. D., Calders, K., Chapman, C., Chapman, H., Comiskey, J., de Haulleville, T., Decuyper, M., DeVries, B., Dolezal, J., Droissart, V., Ewango, C., Feyera, S., Gebrekirstos, A., Gereau, R., Gilpin, M., Hakizimana, D., Hall, J., Hamilton, A., Hardy, O., Hart, T., Heiskanen, J., Hemp, A., Herold, M., Hiltner, U., Horak, D., Kamdem, M. N., Kayijamahe, C., Kenfack, D., Kinyanjui, M. J., Klein, J., Lisingo, J., Lovett, J., Lung, M., Makana, J. R., Malhi, Y., Marshall, A., Martin, E. H., Mitchard, E. T. A., Morel, A., Mukendi, J. T., Muller, T., Nchu, F., Nyirambangutse, B., Okello, J., Peh, K. S. H., Pellikka, P., Phillips, O. L., Plumptre, A., Qie, L., Rovero, F., Sainge, M. N., Schmitt, C. B., Sedlacek, O., Ngute, A. S. K., Sheil, D., Sheleme, D., Simegn, T. Y., Simo-Droissart, M., Sonké, B., Soromessa, T., Sunderland, T., Svoboda, M., Taedoumg, H., Taplin, J., Taylor, D., Thomas, S. C., Timberlake, J., Tuagben, D., Umunay, P., Uzabaho, E., Verbeeck, H., Vleminckx, J., Wallin, G., Wheeler, C., et al.: High aboveground carbon stock of African tropical montane forests, Nature, 596, 536–542, https://doi.org/10.1038/s41586-021-03728-4, 2021.

Cuni-Sanchez, A., Martin, E. H., Uzabaho, E., Ngute, A. S. K., Bitariho, R., Kayijamahe, C., Marshall, A. R., Mohamed, N. A., Mseja, G. A., Nkwasibwe, A., Rovero, F., Sheil, D., Tinkasimire, R., Tumugabirwe, L., Feeley, K. J., and Sullivan, M. J. P.: Evidence of thermophilization in Afromontane forests, Nature Communications, 15, https://doi.org/10.1038/s41467-024-48520-w, 2024.

Duque, A., Stevenson, P. R., and Feeley, K. J.: Thermophilization of adult and juvenile tree communities in the northern tropical Andes, Proceedings of the National Academy of Sciences of the United States of America, 112, 10744–10749, https://doi.org/10.1073/pnas.1506570112, 2015.

Duque, A., Peña, M. A., Cuesta, F., González-Caro, S., Kennedy, P., Phillips, O. L., Calderón-Loor, M., Blundo, C., Carilla, J., Cayola, L., Farfán-Ríos, W., Fuentes, A., Grau, R., Homeier, J., Loza-Rivera, M. I., Malhi, Y., Malizia, A., Malizia, L., Martínez-Villa, J. A., Myers, J. A., Osinaga-Acosta, O., Peralvo, M., Pinto, E., Saatchi, S., Silman, M., Tello, J. S., Terán-

Valdez, A., and Feeley, K. J.: Mature Andean forests as globally important carbon sinks and future carbon refuges, Nature Communications, 12, 1–10, https://doi.org/10.1038/s41467-021-22459-8, 2021.

Dusenge, M. E., Wittemann, M., Mujawamariya, M., Ntawuhiganayo, E. B., Zibera, E., Ntirugulirwa, B., Way, D. A., Nsabimana, D., Uddling, J., and Wallin, G.: Limited thermal acclimation of photosynthesis in tropical montane tree species, Global Change Biology, 27, 4860–4878, https://doi.org/10.1111/gcb.15790, 2021.

Dusenge, M. E., González-Caro, S., Restrepo, Z., Gardner, A., Meir, P., Hartley, I. P., Sitch, S., Sanchez, A., Villegas, J. C., and Mercado, L. M.: Unexpected Large Photosynthetic Thermal Plasticity of Montane Andean Trees, Global Change Biology, 31, e70266, https://doi.org/10.1111/gcb.70266, 2025.

Duursma, R. A.: Plantecophys - An R package for analysing and modelling leaf gas exchange data, PLoS ONE, 10, 1–13, https://doi.org/10.1371/journal.pone.0143346, 2015.

Fadrique, B., Báez, S., Duque, Á., Malizia, A., Blundo, C., Carilla, J., Osinaga-Acosta, O., Malizia, L., Silman, M., Farfán-Ríos, W., Malhi, Y., Young, K. R., Cuesta C, F., Homeier, J., Peralvo, M., Pinto, E., Jadan, O., Aguirre, N., Aguirre, Z., and Feeley, K. J.: Widespread but heterogeneous responses of Andean forests to climate change, Nature, 564, 207–212, https://doi.org/10.1038/s41586-018-0715-9, 2018.

Fisher, R. A., Koven, C. D., Anderegg, W. R. L., Christoffersen, B. O., Dietze, M. C., Farrior, C. E., Holm, J. A., Hurtt, G. C., Knox, R. G., Lawrence, P. J., Lichstein, J. W., Longo, M., Matheny, A. M., Medvigy, D., Muller-Landau, H. C., Powell, T. L., Serbin, S. P., Sato, H., Shuman, J. K., Smith, B., Trugman, A. T., Viskari, T., Verbeeck, H., Weng, E., Xu, C., Xu, X., Zhang, T., and Moorcroft, P. R.: Vegetation demographics in Earth System Models: A review of progress and priorities, Global Change Biology, 24, 35–54, https://doi.org/10.1111/gcb.13910, 2018.

Fyllas, N. M., Bentley, L. P., Shenkin, A., Asner, G. P., Atkin, O. K., Díaz, S., Enquist, B. J., Farfan-Rios, W., Gloor, E., Guerrieri, R., Huasco, W. H., Ishida, Y., Martin, R. E., Meir, P., Phillips, O., Salinas, N., Silman, M., Weerasinghe, L. K., Zaragoza-Castells, J., and Malhi, Y.: Solar radiation and functional traits explain the decline of forest primary productivity along a tropical elevation gradient, Ecology Letters, 20, 730–740, https://doi.org/10.1111/ele.12771, 2017.

González-Caro, S., Tello, J. S., Myers, J. A., Feeley, K., Blundo, C., Calderón-Loor, M., Carilla, J., Cayola, L., Cuesta, F., Farfán, W., Fuentes, A. F., Garcia-Cabrera, K., Grau, R., Idarraga, Á., Loza, M. I., Malhi, Y., Malizia, A., Malizia, L., Osinaga-Acosta, O., Pinto, E., Salinas, N., Silman, M., Terán-Valdéz, A., and Duque, Á.: Historical Assembly of Andean Tree Communities, Plants, 12, https://doi.org/10.3390/plants12203546, 2023.

Guo, Z., Yan, Z., Majcher, B. M., Lee, C. K. F., Zhao, Y., Song, G., Wang, B., Wang, X., Deng, Y., Michaletz, S. T., Ryu, Y., Ashton, L. A., Lam, H. M., Wong, M. S., Liu, L., and Wu, J.: Dynamic biotic controls of leaf thermoregulation across the diel timescale, Agricultural and Forest Meteorology, 315, 108827, https://doi.org/10.1016/j.agrformet.2022.108827, 2022.

Harper, A. B., Wiltshire, A. J., Cox, P. M., Friedlingstein, P., Jones, C. D., Mercado, L. M., Sitch, S., Williams, K., and Duran-Rojas, C.: Vegetation distribution and terrestrial carbon cycle in a carbon cycle configuration of JULES4.6 with new plant functional types, Geoscientific Model Development, 11, 2857–2873, https://doi.org/10.5194/gmd-11-2857-2018, 2018.

Knauer, J., Cuntz, M., Smith, B., Canadell, J. G., Medlyn, B. E., Bennett, A. C., Caldararu, S., and Haverd, V.: Higher global gross primary productivity under future climate with more advanced representations of photosynthesis, Science Advances, 9, 24–28, https://doi.org/10.1126/SCIADV.ADH9444, 2023.

Kumarathunge, D. P., Medlyn, B. E., Drake, J. E., Tjoelker, M. G., Aspinwall, M. J., Battaglia, M., Cano, F. J., Carter, K. R., Cavaleri, M. A., Cernusak, L. A., Chambers, J. Q., Crous, K. Y., De Kauwe, M. G., Dillaway, D. N., Dreyer, E., Ellsworth, D. S., Ghannoum, O., Han, Q., Hikosaka, K., Jensen, A. M., Kelly, J. W. G., Kruger, E. L., Mercado, L. M., Onoda, Y., Reich,

P. B., Rogers, A., Slot, M., Smith, N. G., Tarvainen, L., Tissue, D. T., Togashi, H. F., Tribuzy, E. S., Uddling, J., Vårhammar, A., Wallin, G., Warren, J. M., and Way, D. A.: Acclimation and adaptation components of the temperature dependence of plant photosynthesis at the global scale, New Phytologist, 222, 768–784, https://doi.org/10.1111/nph.15668, 2019.

Lin, Y. S., Medlyn, B. E., Duursma, R. A., Prentice, I. C., Wang, H., Baig, S., Eamus, D., De Dios, V. R., Mitchell, P., Ellsworth, D. S., De Beeck, M. O., Wallin, G., Uddling, J., Tarvainen, L., Linderson, M. L., Cernusak, L. A., Nippert, J. B., Ocheltree, T. W., Tissue, D. T., Martin-StPaul, N. K., Rogers, A., Warren, J. M., De Angelis, P., Hikosaka, K., Han, Q., Onoda, Y., Gimeno, T. E., Barton, C. V. M., Bennie, J., Bonal, D., Bosc, A., Löw, M., Macinins-Ng, C., Rey, A., Rowland, L., Setterfield, S. A., Tausz-Posch, S., Zaragoza-Castells, J., Broadmeadow, M. S. J., Drake, J. E., Freeman, M., Ghannoum, O., Hutley, L. B., Kelly, J. W., Kikuzawa, K., Kolari, P., Koyama, K., Limousin, J. M., Meir, P., Da Costa, A. C. L., Mikkelsen, T. N., Salinas, N., Sun, W., and Wingate, L.: Optimal stomatal behaviour around the world, Nature Climate Change, 5, 459–464, https://doi.org/10.1038/nclimate2550, 2015.

Maréchaux, I., Fischer, F. J., Schmitt, S., and Chave, J.: TROLL 4 . 0 : representing water and carbon fluxes , leaf phenology and intraspecific trait variation in a mixed-species individual-based forest dynamics model – Part 1 : Model description, 2024.

Marthews, T. R., Malhi, Y., Girardin, C. A. J., Silva Espejo, J. E., Aragão, L. E. O. C., Metcalfe, D. B., Rapp, J. M., Mercado, L. M., Fisher, R. A., Galbraith, D. R., Fisher, J. B., Salinas-Revilla, N., Friend, A. D., Restrepo-Coupe, N., and Williams, R. J.: Simulating forest productivity along a neotropical elevational transect: Temperature variation and carbon use efficiency, Global Change Biology, 18, 2882–2898, https://doi.org/10.1111/j.1365-2486.2012.02728.x, 2012.

Martínez, R., Ruiz, D., Andrade, M., Blacutt, L., and Pabón, D.: Synthesis of the Climate of the Tropical Andes BT - Climate Change and Biodiversity in the Tropical Andes, Climate Change and Biodiversity in the Tropical Andes, 97–109, 2011.

Medlyn, B. E., Dreyer, E., Ellsworth, D., Forstreuter, M., Harley, P. C., Kirschbaum, M. U. F., Le Roux, X., Montpied, P., Strassemeyer, J., Walcroft, A., Wang, K., and Loustau, D.: Temperature response of parameters of a biochemically based model of photosynthesis. II. A review of experimental data, Plant, Cell and Environment, 25, 1167–1179, https://doi.org/10.1046/j.1365-3040.2002.00891.x, 2002.

Medlyn, B. E., Duursma, R. A., Eamus, D., Ellsworth, D. S., Prentice, I. C., Barton, C. V. M., Crous, K. Y., De Angelis, P., Freeman, M., and Wingate, L.: Reconciling the optimal and empirical approaches to modelling stomatal conductance, Global Change Biology, 17, 2134–2144, https://doi.org/10.1111/j.1365-2486.2010.02375.x, 2011.

Mercado, L. M., Medlyn, B. E., Huntingford, C., Oliver, R. J., Clark, D. B., Sitch, S., Zelazowski, P., Kattge, J., Harper, A. B., and Cox, P. M.: Large sensitivity in land carbon storage due to geographical and temporal variation in the thermal response of photosynthetic capacity, New Phytologist, 218, 1462–1477, https://doi.org/10.1111/nph.15100, 2018.

Montaño-Centellas, F., Fuentes, A. F., Cayola, L., Macía, M. J., Arellano, G., Loza, M. I., Nieto-Ariza, B., and Tello, J. S.: Elevational range sizes of woody plants increase with climate variability in the Tropical Andes, Journal of Biogeography, 51, 814–826, https://doi.org/10.1111/jbi.14783, 2024.

Mujawamariya, M., Wittemann, M., Dusenge, M. E., Manishimwe, A., Ntirugulirwa, B., Zibera, E., Nsabimana, D., Wallin, G., and Uddling, J.: Contrasting warming responses of photosynthesis in early- and late-successional tropical trees, Tree Physiology, 43, 1104–1117, https://doi.org/10.1093/treephys/tpad035, 2023.

Myers, N., Russell, M. A., Mittermeier, C. G., Fonseca, G. A. B. da, Kent, J., Mittermeier, R. A., Mittermeier, C. G., Fonseca, G. A. B. da, and Kent, J.: Biodiversity hotspots for conservation priorities Norman, Nature, 403, 854–858, 2010.

Oliver, R. J., Mercado, L. M., Clark, D. B., Huntingford, C., Taylor, C. M., Vidale, P. L., McGuire, P. C., Todt, M., Folwell, S., Shamsudheen Semeena, V., and Medlyn, B. E.: Improved representation of plant physiology in the JULES-vn5.6 land

surface model: photosynthesis, stomatal conductance and thermal acclimation, Geoscientific Model Development, 15, 5567–5592, https://doi.org/10.5194/gmd-15-5567-2022, 2022.

Poulter, B., Ciais, P., Hodson, E., Lischke, H., Maignan, F., Plummer, S., and Zimmermann, N. E.: Plant functional type mapping for earth system models, Geoscientific Model Development, 4, 993–1010, https://doi.org/10.5194/gmd-4-993-2011, 2011.

Puy, A., Becker, W., Lo Piano, S., and Saltelli, A.: a Comprehensive Comparison of Total-Order Estimators for Global Sensitivity Analysis, International Journal for Uncertainty Quantification, 12, 1–18, https://doi.org/10.1615/Int.J.UncertaintyQuantification.2021038133, 2022.

Siefert, A., Violle, C., Chalmandrier, L., Albert, C. H., Taudiere, A., Fajardo, A., Aarssen, L. W., Baraloto, C., Carlucci, M. B., Cianciaruso, M. V., de L. Dantas, V., de Bello, F., Duarte, L. D. S., Fonseca, C. R., Freschet, G. T., Gaucherand, S., Gross, N., Hikosaka, K., Jackson, B., Jung, V., Kamiyama, C., Katabuchi, M., Kembel, S. W., Kichenin, E., Kraft, N. J. B., Lagerström, A., Bagousse-Pinguet, Y. Le, Li, Y., Mason, N., Messier, J., Nakashizuka, T., Overton, J. M., Peltzer, D. A., Pérez-Ramos, I. M., Pillar, V. D., Prentice, H. C., Richardson, S., Sasaki, T., Schamp, B. S., Schöb, C., Shipley, B., Sundqvist, M., Sykes, M. T., Vandewalle, M., and Wardle, D. A.: A global meta-analysis of the relative extent of intraspecific trait variation in plant communities, Ecology Letters, 18, 1406–1419, https://doi.org/10.1111/ele.12508, 2015.

Smith, M. N., Taylor, T. C., van Haren, J., Rosolem, R., Restrepo-Coupe, N., Adams, J., Wu, J., de Oliveira, R. C., da Silva, R., de Araujo, A. C., de Camargo, P. B., Huxman, T. E., and Saleska, S. R.: Empirical evidence for resilience of tropical forest photosynthesis in a warmer world, Nature Plants, 6, 1225–1230, https://doi.org/10.1038/s41477-020-00780-2, 2020.

Smith, N. G., Keenan, T. F., Colin Prentice, I., Wang, H., Wright, I. J., Niinemets, Ü., Crous, K. Y., Domingues, T. F., Guerrieri, R., Yoko Ishida, F., Kattge, J., Kruger, E. L., Maire, V., Rogers, A., Serbin, S. P., Tarvainen, L., Togashi, H. F., Townsend, P. A., Wang, M., Weerasinghe, L. K., and Zhou, S.-X.: Global photosynthetic capacity is optimized to the environment, Ecology Letters, 22, 506–517, https://doi.org/10.1111/ele.13210, 2019.

van de Weg, M. J., Meir, P., Grace, J., and Ramos, G. D.: Photosynthetic parameters, dark respiration and leaf traits in the canopy of a Peruvian tropical montane cloud forest, Oecologia, 168, 23–34, https://doi.org/10.1007/s00442-011-2068-z, 2012.

van de Weg, M. J., Meir, P., Williams, M., Girardin, C., Malhi, Y., Silva-Espejo, J., and Grace, J.: Gross Primary Productivity of a High Elevation Tropical Montane Cloud Forest, Ecosystems, 17, 751–764, https://doi.org/10.1007/s10021-014-9758-4, 2014.

Yan, Z., Sardans, J., Peñuelas, J., Detto, M., Smith, N. G., Wang, H., Guo, L., Hughes, A. C., Guo, Z., Lee, C. K. F., Liu, L., and Wu, J.: Global patterns and drivers of leaf photosynthetic capacity: The relative importance of environmental factors and evolutionary history, Global Ecology and Biogeography, 1–15, https://doi.org/10.1111/geb.13660, 2023.

Zaka, S., Frak, E., Julier, B., Gastal, F., and Louarn, G.: Intraspecific variation in thermal acclimation of photosynthesis across a range of temperatures in a perennial crop, AoB PLANTS, 8, https://doi.org/10.1093/aobpla/plw035, 2016.

Acknowledgements

SGC, MED, ZRC, AJFC, IH, PM, AS, DR and LMM acknowledge funding from the UK Natural Environment Research Council (NE/R001928/1). SGC, ZR, IH, PM, and LMM acknowledge funding from the UK Natural Environment Research

Council (NE/X001172/1.) For the purpose of open access, the author has applied a ‘Creative Commons Attribution (CC BY) licence to any Author Accepted Manuscript version arising from this submission

Author contributions

SGC and LMM conceptualized this study. Data were collected by MED, ZR, AJFC, AS, SGC and LMM. LMM, IH and PM with support from AS, DR and ZR wrote the grant that funded the project that funded the work and collected the data. SGC analysed data. SGC drafted the manuscript with significant inputs from LMM, IH and PM. All authors provided inputs to the final version of the manuscript.

Figure S1. Comparison between observed and modeled photosynthesis and modeled diurnal variation of net CO_2 assimilation for montane and lowland species. (A) Relationship between observed and modeled daily carbon assimilation (A_{net}) showing a strong agreement between both estimates. (B) Modeled diurnal variation of photosynthesis for montane species under environmental conditions at the 14°C site (blue) and the 22°C site (red). (C) Modeled diurnal variation of photosynthesis for lowland species under the same environmental conditions (blue = 14°C; red = 22°C).

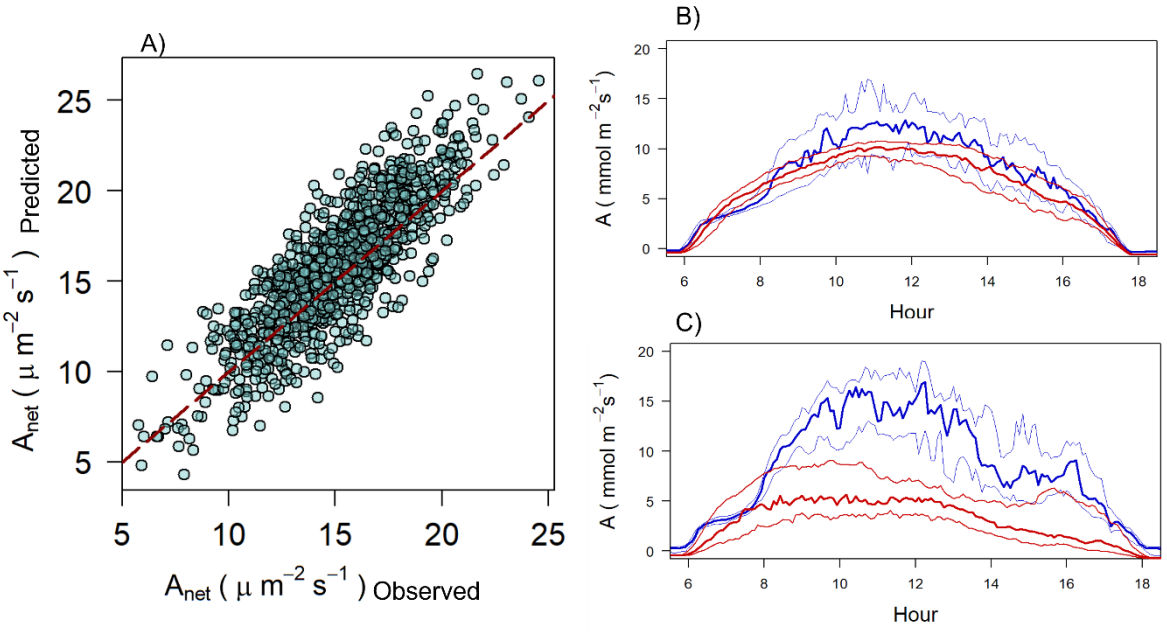

Figure S2. Boxplot of simulated parameter distribution of analysed species for V_{cmax} (a), J_{max} (b) and g_1 (b). Blue boxes represent montane species, and red boxes represent lowland species and the 14°C site (1) and at the 22°C site (2).

a)
V_{cmax} (μ mol m^{-1} s^{-1})
0
50
100
150
200
250
b)
J_{max} (μ mol m^{-1} s^{-1})
0
5
10
15
20
c)
g_1 (μ mol m^{-1} s^{-1})
0
5
10
15
20
1.I.marginata
2.I.marginata
1.I.spectabilis
2.I.spectabilis
1.C.multiflora
2.C.multiflora
1.Q.humboldtii
2.Q.humboldtii
1.M.theizans
2.M.theizans
1.C.fagifolia
2.C.fagifolia
1.W.pubescens
2.W.pubescens
1.T.lepidota
2.T.lepidota

Figure S3. Residuals of observed and predicted leaf-level photosynthesis relative to intercellular CO_2 concentration (Ci), photosynthetic active radiation (PAR), air temperature (Tair), and vapor pressure deficit (VPD) for simulations at the 14°C (top row) and 22°C sites (bottom row). The plots also show the range of environmental conditions used in the simulations and sensitivity analyses: Ci = 50–1200 µmol mol^{-1}, PAR = 0–2000 µmol m^{-2} s^{-1}, Tair = 10–30°C, and VPD = 0.2–2.5 kPa.